Debris Clouds behind Plates Impacted by Hypervelocity Pellets

H. F. Swift,* D. D. Preonas, and W. C. Turpin†
University of Dayton Research Institute, Dayton, Ohio

AND

J. M. Carson‡
Air Force Materials Laboratory, Wright-Patterson Air Force Base, Ohio

The effectiveness of two-plate meteoroid shields is determined by the character of the debris cloud ejected behind the front plate after a hypervelocity impact. The material velocities, distributions, and momentum intensities of these clouds have been determined experimentally for 6061-T6 aluminum, OFHC copper, and cadmium pellets impacting optimal thickness bumpers of the same materials at 7.0 km/sec. Debris dissection techniques, free suspended flyer plates, flash radiography, and high speed photography were used to make these measurements. The results were compared with numerical computations from a computer code that describes thin plate impacts as two-dimensional flow processes. Agreement was reasonably good with respect to debris trajectory, origin, and velocity comparisons (except for the Cd pellets), but predicted momentum profiles failed to agree with experiments near the cloud axes, and predicted cloud thicknesses were too great in all cases. On the whole, the discrepancies were considered to be sufficient to call into question any shield design based solely on the code predictions.

Background

TWO primary approaches are currently available for predicting the responses of spaced-plate shields to meteoroid impacts: 1) use of numerical analyses (computater codes that treat hypervelocity impacts as two-dimensional material-flow processes) and 2) extrapolation of the results of experimental impact data generated at lower velocities. Because the latter extrapolations require questionable assumptions regarding similarity of impact effects at different velocity regimes, and whereas the computer codes deal directly with the velocities of interest and are based on relatively plausible assumptions concerning materials response, the codes have been used widely in the design of meteoroid protection systems. In the present study, a typical code§ was used to predict general dynamic characteristics of clouds generated behind thin plates (bumpers) that were impacted by pellets traveling at velocities achievable with laboratory facilities.[2] Particular impact situations were chosen to simulate the phenomena that are thought to be most important during actual encounters between meteoroids and spaced shields. These impact situations were then produced experimentally, the dynamic parameters were measured, and the results were compared with the code predictions. Results from this study are useful both for establishing the reliability of this code and other similar codes, and for guiding the development of more advanced versions with greater reliability.

Presented as Paper 69-380 at the AIAA Hypervelocity Impact Conference Cincinnati, Ohio, April 30–May 2; submitted May 2, 1969; revision received October 16, 1969. The authors wish to acknowledge and thank the following persons: L. Shiverdecker, H. Taylor, and E. Strader, who assisted in the collection of much of the experimental data reported in this article; and J. H. Cunningham, who gathered a significant portion of the experimental data on cloud momentum as part of his thesis project for the Air Force Institute of Technology.[1]

* Head, Physics of Materials Group.
† Staff Engineer
‡ Captain U.S. Air Force.

§ "STEEP," Shock Hydrodynamics Inc., Sherman Oaks, California.

Experiments

The principal goals of this investigation were to establish the velocity, mass, and momentum distributions of debris clouds ejected behind thin plates. In addition, the precise trajectories and initial positions of materials that form each part of the debris clouds were to be determined. The experimental impact cases were chosen to correspond with those examined with the code. In each case, spherical pellets were projected against extensive plates of the same material whose thicknesses were $\frac{1}{4}$ the pellet diameter. Theoretical studies have shown that this ratio between plate thickness and pellet diameter produces the highest average pressures in the pellet and plate material that is injected into the highly destructive portions of the debris clouds.[3]

Three materials were selected: 6061-T6 aluminum, because previous investigations indicated that the resulting debris is in an incipient molten condition at impact velocities of 7.0 km/sec (Refs. 4 and 5); OFHC copper, because its debris should be completely molten at these velocities; and cadmium, because its debris clouds are vaporous.[4] Pellets 3.18 mm in diam were used with 0.79-mm-thick targets of the same material in the case of cadmium and OFHC copper. The material distribution study of aluminum clouds required a degree of radiograph resolution not attainable with the standard size pellet. In this instance, the impact geometry was scaled up to double size, i.e., 6.35-mm pellets impacting 1.58-mm targets. Experimental impact velocities throughout the investigation were in the range of 6.9 to 7.2 km/sec.

Relatively little information can be gained by observing uninterrupted debris clouds as they expand, since their leading edges are quite smooth and they are often opaque. These limitations have been overcome by inserting solid elements into the paths of expanding debris clouds to interrupt or delay parts of the clouds. The effects upon the subsequent motion of the undisturbed cloud elements are then observed both radiographically with flash x-ray, and optically with framing camera equipment. In this way, the speeds and directions of separated cloud elements can be determined directly, as can the distribution of material within clouds. Individual experimental requirements dictate the particular characteristics of the "cloud dissection" equipment.

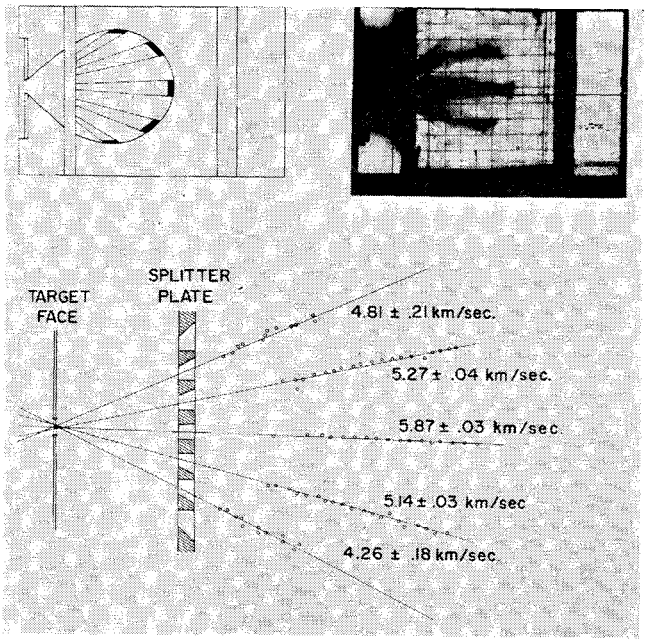

Fig. 1 Debris cloud dissection technique showing typical results from Beckman & Whitley 300 framing camera.

Cloud Velocity Profiles

During early cloud dissection experiments, the clouds were intersected by plates mounted perpendicular to the axis of the undisturbed clouds, with lines of rectangular holes extending across the cloud axis (see Fig. 1). Considerable care was taken in the design of the plates to prevent material from rebounding off of the hole walls. However, only five or six cloud components could be observed during each experiment. This limitation was relieved during later tests, by using slots instead of holes in the cloud dissection plates. Steel wires 0.75 mm in diam were spaced 4 mm apart across each slot. Clouds that expanded through these dissection plates were divided into as many as 15 segments whose speeds and directions of travel could be determined independently.

Sequences of 12–30 frames of the expanding debris cloud elements after dissection were taken with a rotating mirror framing camera (Beckman & Whitley Model 300). The positions of as many as 50 points from each frame image were measured on an automatic film reader that printed x and y coordinates of the points. The position data were corrected automatically to remove systematic camera errors and were least squares fitted to element position vs time plots. These plots yield flow direction and speed of the respective cloud elements. Thus, the velocities of the leading edges of the debris clouds were obtained. The velocity components along lines parallel to the cloud axis are compared with code predictions in Fig. 2. Error bars on the experimental points represent one standard deviation of uncertainty in element velocity and trajectory angle. Since the experimental pellet velocities were near 7.0 km/sec, whereas the code predictions had been generated for impact velocities of 7.5 km/sec, all debris cloud velocity component data, both experimental and predicted, were normalized by dividing by their respective pellet velocities.

For aluminum and copper, the observed and predicted results are in reasonable accord between off-axis angles β of $4° \lesssim \beta \lesssim 20°$. At $\beta > 20°$, the predicted axial velocities are low, and at $\beta < 4°$, they are high. The code, however, was not expected to be accurate very near the axis due to numerical difficulties. Both of these discrepancies will alter the predicted cloud position significantly as time progresses and thus affect the material distribution within the cloud, as discussed later. For cadmium, the predicted curve lies considerably above the experimental data at all angles, and its shape is different from that of a curve one might draw through the data.

Cloud Material Trajectories

The cloud velocity measurements described previously provide only approximate information on the trajectories of debris cloud material. To obtain more precise data on the directions of debris elements and the positions in the impact plate from which the material originated, it was necessary to intercept the debris clouds with a structure that had many points whose positions could be determined accurately, and then observe the motions of corresponding points on the debris cloud during subsequent expansion. A precise 6.35 mm × 6.35 mm grid of 0.5-mm-diam copper wires was mounted 5 cm behind plates to be impacted. The expanding debris clouds were selectively interrupted by the wires and expanded another 10 cm behind the grid before impacting a plexiglas witness plate. A particle shadow of the grid was formed on the witness plate. Figure 3 shows such a plate with a typical shadow. The grid, witness plate, and impacted target plate were aligned with the cross-hairs of a telescope mounted on the range axis so that a three-dimensional coordinate system enclosing all the experimental equipment could be established. The position of 70 to 120 intersections of the grid shadow on the witness plate and the corresponding intersection points of the actual grid were measured with respect to this coordinate system. The data reduction consisted of establishing lines in space that pass through corresponding intersections of the grid and its shadow, and extrapolating these lines back to the region of the impacted plates.

Cloud trajectory data were reduced in two forms: first, the apparent debris origin on the plane of the target plate rear surface was located; and second, the validity and

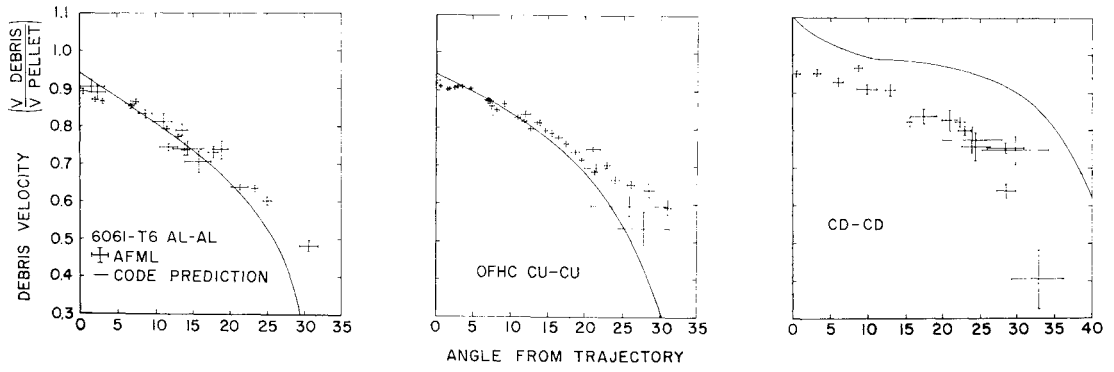

Fig. 2 Axial debris velocity profiles.

possible location of a single emanating point for all debris was established. Figure 4 shows the extrapolated origin of cloud debris in the rear surface plane of the target plate as experimentally determined for all three materials. In all cases the debris collected on the witness plates, in particular the inner cone debris, appears to originate from an area on the plate of about the same size as the original cross-sectional area of the pellet. The inner cone of debris generates a discernible area of primary damage on the impacted plates. This inner cone contains the energetic particles comprising most of the damage potential of the debris cloud.[6]

Experimental results indicate the existence of minimum emanating areas for the debris that are significantly smaller than the cross sections of the impacting pellets. Isometric graphs showing the location of these areas uprange of the impacted plate for aluminum, copper, and cadmium are presented in Fig. 5. Each line on the graphs represents measured data, and each graph pertains to a single experiment. The results have been reproduced on successive tests to within 200 μ, however.

For each impact situation, the code identified three different types of debris that originated from separate areas in the target plate. The highly energetic debris contained in the central portion of the cloud came from a circular area in the plate centered on the impact point; this area was somewhat smaller than that of the pellet cross-section. Less energetic debris toward the edges of the main cloud structure originated from an annular ring of "necking" in the plate adjacent to the central area. At later times, very low energy debris that formed the fringes of debris clouds came from a second annular ring that extended out to near the final hole diameter. Experimental techniques primarily treated the energetic debris in the central portion of the cloud.

Table 1 compares code-predicted and experimental results covering the location and character of a debris emanating point (or area) for aluminum, copper, and cadmium debris clouds. Distances from the impacted plate were meaured along the pellet trajectory uprange from the rear surface of the target plate. Separation distance of the emanating area from the impacted plate is thus equal to the listed distance minus the plate thickness. The two-dimensional nature of the code predictions constrained all predicted velocity vectors to intersect the cloud axis. Therefore, they generated a "line" of debris origin along the cloud axis. Extrapolated velocity vectors indicated separate emanation areas along the cloud axis that corresponded to the three predicted types of debris. Shock Hydrodynamics Inc. chose to use a weighted treatment of these points that produced single emanating points with relatively large standard deviations.[2] These points were considered zero areas for purposes of comparison with experimental results in Table 1.

Substantial agreement between code predictions and experimental results pertaining to cloud material trajectories was found within the error limits of both data.

Material Distribution

The distribution of material within debris clouds has been established by dissecting expanding debris clouds after material interactions have become insignificant. Two massive steel jaws were mounted to intersect all of the cloud except a slice across the cloud axis that was allowed to pass unhindered (see Fig. 6). These slices were flash radiographed¶ after subsequent expansion to determine their material density distributions and, hence, the material density distributions within equivalent undisturbed clouds. The front and rear edges of the debris could be observed for some distance off cloud axis in both directions. Bands of relatively high and low material densities were observed within the debris area in some cases. The radiographs were not of sufficient quality, however, to permit quantitative measurements of absolute material density profiles within the clouds.

Material distribution within the debris cloud was determined experimentally for all three materials and compared with code predictions in Fig. 7. Radiographs of cross-sectional debris cloud slices were made at known times after impact, and the positions of leading cloud edges were compared with experimental data from the cloud velocity study

Table 1 Debris emanation area

Material	Area size, pellet areas		Area distance from plate, pellet diameters	
	Experiment	Code	Experiment	Code
Al	0.076	0	1.25	1.29 ± 1.24
Cu	0.101	0	0.93	1.24 ± 1.02
Cd	0.384	0	0.34	0.97 ± 1.07

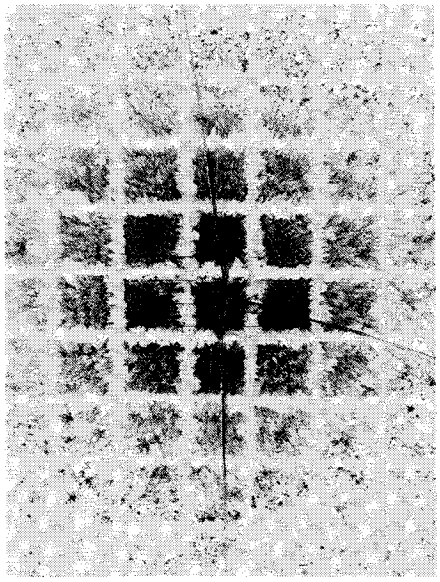

Fig. 3 Plexiglas witness plate with debris generated grid "shadow."

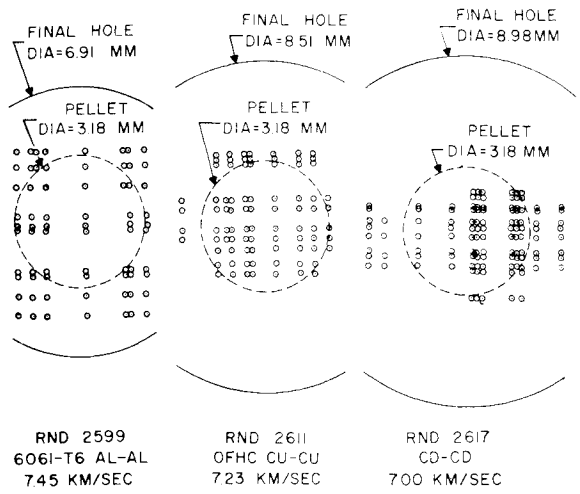

Fig. 4 Debris origin on impacted plates.

¶ Flash radiographs with exposure times below 50 nsec were taken using a Field Emission Type 231 x-ray system.

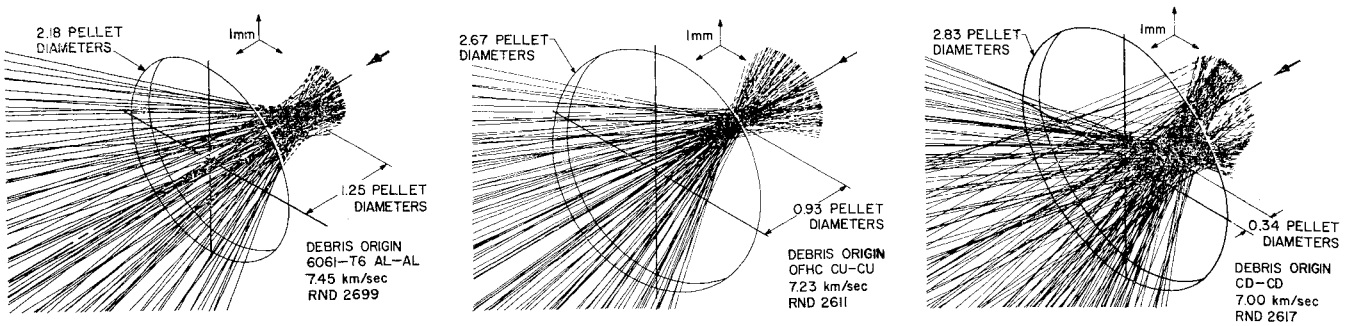

Fig. 5 Debris emanating areas behind impacted plates.

(optical) extrapolated to the same time. This extrapolation was based on experimentally measured cloud velocities and thus provided a check on the validity of both the experimental debris cloud velocity and the material distribution results. All experimental data were normalized to the code velocity of 7.5 km/sec. Leading and trailing edges of the code-predicted cloud were extrapolated in all cases from the last computed cloud profiles (≈ 0.9 μsec after impact).

For aluminum, general agreement between radiograph and optical leading cloud edges exists. In two areas located symmetrically off the cloud axis, the radiograph cloud edge is slightly displaced behind the optical edge, possibly because of differences in optical and radiograph cross sections.

In the region near the cloud axis, the code-predicted leading cloud edge is ahead of the experimental plot, and it comes to a point on the axis. (This point is felt to be the result of the same numerical difficulties mentioned earlier.) As the angle from trajectory increases, the code-predicted leading edge of the cloud intersects the observed leading edge and then falls behind it at an increasing rate. The predicted trailing edge represents a greater departure from experiment. The code predicts a relatively thick cloud, whereas experimental results show a very thin one. (The importance of this discrepancy is discussed later.) For copper, correlation between radiograph and optical leading cloud edges is excellent. The situation with respect to code predictions is similar to that for Al. For Cd, fairly good agreement between radiograph and optical leading cloud edges is achieved, but there is little similarity between the observed and the predicted cloud shape. The predicted leading edge travels too fast; the predicted trailing edge, too slowly. The cloud thickness discrepancies are much more extreme for Cd than for Al or Cu.

The most striking and singularly important difference between all code-predicted and observed debris clouds is the greater thickness of the predicted clouds. The thickness discrepancies indicate that a significant qualitative difference exists between predicted and observed clouds. Predicted densities within these thicknesses vary from one point to another by less than a factor of four; therefore the existence of significant amounts of material dispersed to densities below radiographic resolution is unlikely.

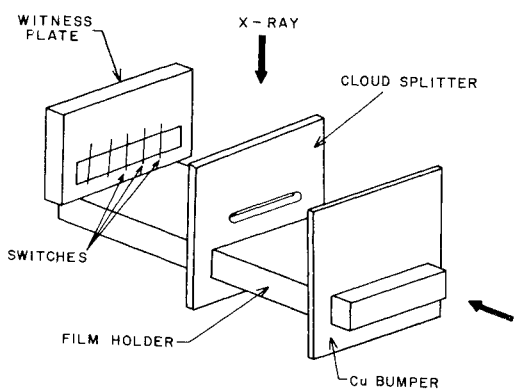

Fig. 6 Debris cloud material distribution experiment.

Cloud Impulse

In principle, there are three quantities related to debris cloud momentum. First is the internal momentum profile of the cloud (i.e. the internal momentum of the cloud per unit solid angle as a function of angle off cloud axis). The second is the momentum felt by small plates in the path of the expanding cloud. This momentum consists of internal cloud momentum plus the momentum of material rebounding off the plates. Finally, there is the momentum transferred to a large plate that interrupts lateral expansion of the cloud. The momentum experienced by such a plate is that received by the small plates plus impulse derived from the relatively long-term pressures generated against the large plate by cloud stagnation. The bulk of measurements made on this (cloud impulse) phase of the theoretical-experimental comparison were of the second and third types.[1]

To measure the momentum of the expanding cloud, small metal plates called flyers (6.0 mm $\times$ 6.0 mm $\times$ 1.5 mm) were suspended lightly behind target plates in a line intersecting the cloud axis and perpendicular to it. The expanding clouds enveloped the flyers and transferred momentum to them, which was evaluated after the cloud passed by monitoring the flyers' recoil velocities with a 26,000 frame/sec camera (Beckman & Whitley Dynafax Model 319B). The momentum of each flyer consisted of the internal momentum of the cloud element subtended by the flyer, plus that due to material rebounding from the impacted flyer surface. Up to 14 separate measurements of debris cloud momentum were determined per test, using this technique. Several tests were made to verify the validity of the results. Flyers of several thicknesses were used and various spacings between the lines of flyers and the original target plates were checked. All of the data for each impact situation checked, after normalization, to within its internal scatter.

Another set of experiments was carried out to evaluate the effects of over-all cloud stagnation. Flyer plates were mounted within holes in a massive steel plate exposed to expanding debris clouds. The flyers experienced the impulse from the cloud stagnation in addition to the impulse absorbed by the freely suspended flyers. Other tests were run where the flyers were mounted behind the holes in the cloud dissection plate. All the data from these tests were superimposed onto plots from the freely suspended flyers data without noticeable effect. These results indicate that the impulse generated by cloud stagnation is relatively slight for the impact situations considered.

Figure 8 compares distributions (total pellet momentum divided by pellet cross-sectional area) in planes 10.16 cm behind target plates. The scatter of the experimental data does not represent measurement error, but is an indication of cloud nonreproducibility. The actual error bars associated with the experimental points are smaller than the symbol

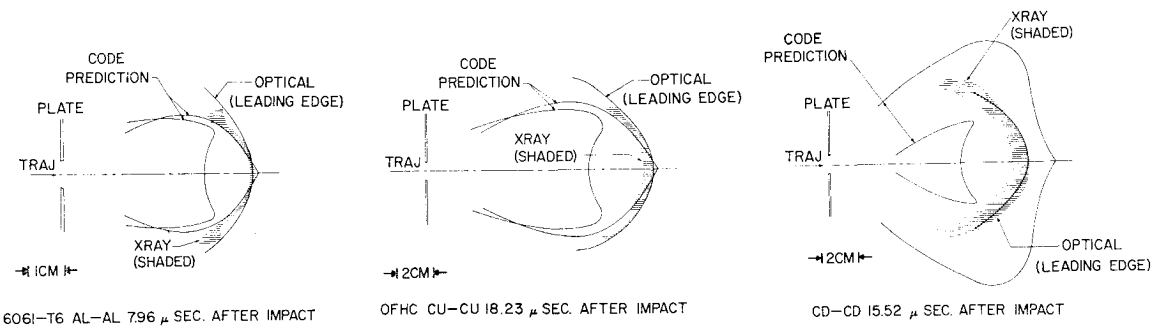

Fig. 7 Debris cloud material distribution.

used to represent the points. The noncontinuous nature of debris clouds causes discrete differences between the material striking given flyer plates identically positioned in multiple impact situations. The effect is least evident in the primarily gaseous debris generated by cadmium impacts, as is clearly shown by the relatively small scatter of the cadmium data.

Aluminum, copper, and cadmium show similar trends in agreement between code-predicted and experimental flyer results. At relatively large off-axis angles ($\beta > 10°$) there is relatively good agreement; the predicted curves fall slightly below the experimental ones, which is to be expected as a result of material rebound effects. For $\beta < 10°$, however, the predicted curves fall farther below the observed curves. For $0 \leq \beta \lesssim 7°$, the code predicts decreases in momentum intensity with decreasing β, while the experimental results increase monotonically. Discontinuous points in the momentum distribution as predicted by the code are not evident within the resolution of experimental data. However, concentric variations were noted in the character of damage on plates exposed to debris impact at about the locations of code-predicted discontinuities. It is not known at this time whether these observed variations in damage are a result of changes in momentum below the resolution of current techniques, changes in the character of the cloud debris, or some combination of these.

Flyer results indicate little or no effect from stagnation pressures (see Al data in Fig. 8), but they include the rebound momentum of material which impacts on them. This additional momentum could give an experimental result up to 1.5 times the internal momentum of the cloud.[7] The experimental curves in Fig. 8 are therefore higher than the true internal momentum intensity of the cloud. The code treats internal momentum, and the known error of the experimental curve implies even better agreement than shown between code and experiment at $\beta > 10°$. At $\beta < 10°$, however, momentum multiplication errors cannot explain the differences in basic trends of the experimental and predicted curves. As a matter of interest, the flyer data give a valid engineering measurement of momentum intensity felt by vehicle structures behind impacted bumpers.

Discussion

In only limited cases did experimental and predicted curves for cloud velocity vs angle agree. Numerical difficulties caused disagreements at $\beta \lesssim 4°$, but more fundamental problems resulted in an excessive rate of decrease in velocity predictions at larger angles for the cases of Cu and Al. The predictions for Cd were too high at all angles. Cloud momentum predictions indicated a leveling off or a reduction of momentum intensity as β was reduced below 10°, while measurements showed monotonic increases in momentum intensity as angles off axis were reduced. Fairly good agreement existed at $\beta > 10°$, however, Finally, measurements indicated that the debris clouds were quite thin, i.e., almost all the debris was confined to a thin shell, while the code predictions showed the debris material dispersed over a sizeable fraction of the cloud volume.

The diversity and scale of these discrepancies appear too extreme to be attributed solely to measurement errors or to computational difficulties. Fundamental errors in experi-

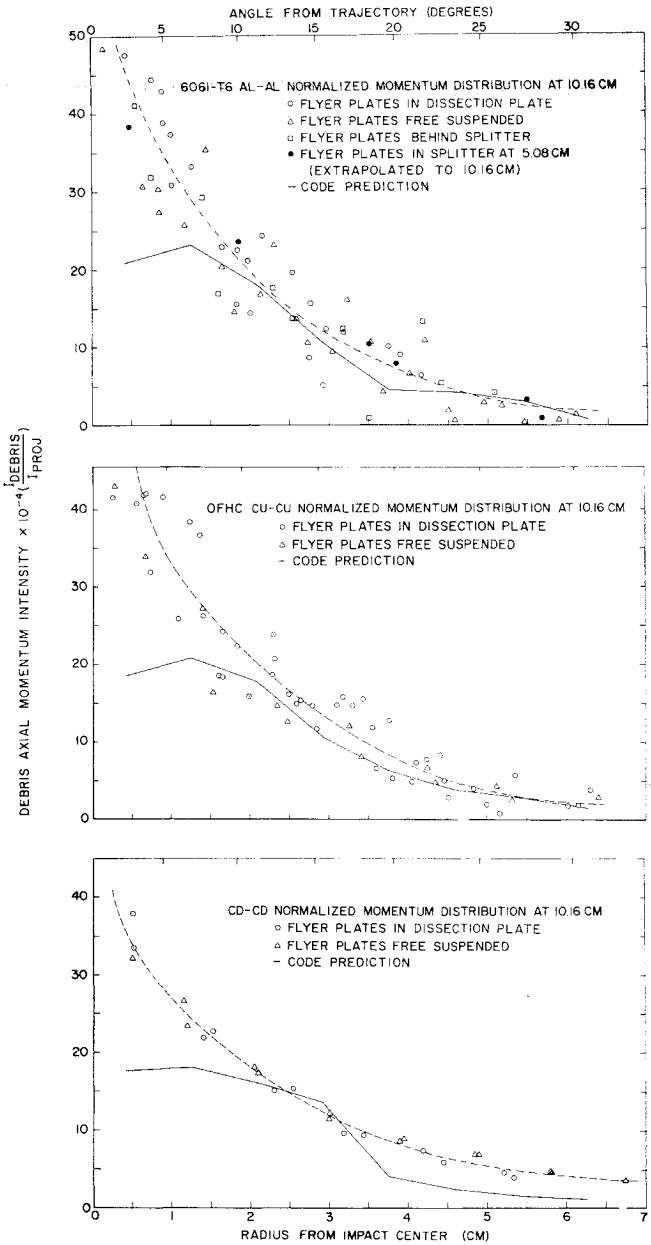

Fig. 8 Debris cloud axial momentum distribution at 10.16 cm.

mental techniques are always a possibility, but seem an unlikely explanation for the discrepancies in this instance for two significant reasons: first, several different techniques were used to gain comparisons with code predictions, and each demonstrated lack of agreement in at least one respect; secondly, the experimental data obtained by the various techniques were mutually consistent within internal scatter. It seems unlikely that all the experimental techniques would be in error and yet correlate with one another.

The possibility arises that the physical model and/or mechanisms on which the computations were based could either be incorrect or not account for some significant processes. For example, the predicted "thick" debris clouds support this possibility. Both the code and experimental data indicate a gaseous debris cloud for the case of the cadmium impacts at 7.5 km/sec. For the model to allow a gaseous cloud, the shock wave reaching the rear surface of the pellet must be strong enough to vaporize it; but this shock must also slow down the material at the rear of the pellet, leading to a thick debris cloud. Conversely, to match the experimental "thin" debris cloud, the shock which reaches the rear of the pellet would be too weak to vaporize it, or the shock wave of necessary strength must turn the pellet material through angles much greater than are predicted by code. This anomaly suggests that one or more processes may be involved in the actual impact situation that are not currently accounted for in the model.

The model used for the code in this case is quite straightforward in its treatment of the high-energy component of the debris cloud material. Conventional shock Hugoniot data for the materials treated is used to compute initial material compression, and well developed equation-of-state data is employed to evaluate the motions of rarefaction fans that attenuate and eventually consume the primary shocks. The very common assumption is made that the expansion of the shock-compressed material is an isentropic process. Recently, this assumption has been called into question.[9] Computational techniques involving entropy trapping were employed to compute the residual energy of the shocked material. This approach is the classic one developed originally for one-dimensional impact situations. It is almost certain that other phenomena make significant contributions to the residual internal energy of material subjected to two-dimensional shock waves, however. One such contribution arises from the massive deformation of the pellet and target material during the early phases of the impact process (which does not occur in one-dimensional impacts). The material is cold-worked by the deformation and is thereby heated. Once material failure has occurred, friction heating takes place as the material elements pass over one another. The importance of any or all of these arguments in resolving the anomaly between experimental and computed results remains to be determined by future examination of the problem.

The next point to be considered is the importance of these discrepancies to the problem at hand—establishing the effectiveness of spaced sheets for protecting vehicles from meteoric impacts. Three fundamental parameters control the response of a sheet to a diffuse impact from a debris cloud: a) momentum intensity distribution, which controls gross plate deformation, plus possible tearing and petalling; b) the cloud thickness, which controls the rate of pressure build-up in the plate material, and hence the characteristics of shock waves generated in the plate, and whether the plate fails via spallation; and c) the size distribution of the debris, which controls the magnitude or existence of cratering damage (this parameter was treated by neither the code nor the reported experiments).

The qualitative divergence between experimental measurements and predictions of momentum intensities indicates that the predicted clouds will not produce a correct representation of deformation-related damage to vehicle hull plates. Incorrect predictions of cloud thicknesses will led to incorrect determinations of spallation damage produced by the clouds. For these reasons, design of shields based on the code alone (without experimental verification) is a hazardous proposition.

The results of this study also point out a more basic problem. Although computational difficulties do exist, the thin plate impact model is one of the simplest treated by two-dimensional impact codes. The bulk of the high-energy material is projected away from the plate before pressures drop to the point where material strength becomes important. By this time, the mean material densities are so low that the material must at least be finely divided such that material strength considerations should remain unimportant.

If the difficulties highlighted by this comparison between code and experiment exist in a relatively simple model, the potential problems in more complicated situations such as thick or laminated plate impacts could be even more serious. It is of obvious importance that the anomalies noted herein be resolved by joint efforts between the experimentalists and theoreticians as quickly as possible so that codes and experimental evaluation techniques that are mutually consistent can be developed. This appears to be a minimum first step in the evolution of computational techniques that can be relied upon in detail to predict impact characteristics at velocities above those achievable in the laboratory.

References

[1] Cunningham, J. H., "Momentum Distribution in the Debris Cloud Produced by Hypervelocity Perforation of Thin Plates," AFML-TR-68-174, July 1968, Air Force Materials Lab., Wright-Patterson Air Force Base, Ohio.

[2] Rosenblatt, M., Kreyenhagen, K. N., and Romine, W. D., "Analytical Study of Debris Clouds Formed by Hypervelocity Impacts of Thin Plates," AFML-TR-68-266, Dec. 1968, Air Force Materials Lab., Wright-Patterson Air Force Base, Ohio.

[3] Tillotson, J. H., "A Theoretical and Experimental Correlation of Hypervelocity Impact on Layered Targets," TR 5-425-R, May 1968, EG&G Corp., Santa Barbara, Calif.

[4] Swift, H. F. and Hopkins, A. K., "The Effects of Bumper Material Properties on the Operation of Spaced Hypervelocity Particle Shields," AFML-TR-68-257, Sept. 1968, Air Force Materials Lab., Wright-Patterson Air Force Base, Ohio.

[5] Olshaker, A. E. and Bjork, R. L., "Hydrodynamics Applied to Hypervelocity Impact," *Proceedings of the Fifth Symposium on Hypervelocity Impact*, Colorado School of Mines, Denver, Colo., Oct. 1961, Vol. 1, Pt. 1, pp. 225–239.

[6] Swift, H. F., Carson, J. M., and Hopkins, A. K., "Ballistic Limits of 6061-T6 Aluminum Bumper Systems," AFML-TR-67-324, Oct. 1967, Air Force Materials Lab., Wright-Patterson Air Force Base, Ohio.

[7] Denardo, B. P. and Nysmith, C. R., "Momentum Transfer and Cratering Phenomena Associated With the Impact of Aluminum Spheres Into Thick Aluminum Targets at Velocities to 24,000 Feet Per Second," *The Fluid Dynamic Aspects of Space Flight*, AGARDograph 87, Vol. 1, Gordon and Breach Science, New York, 1964, pp. 389–402.

[8] Discussions held at the Gordon Research Conference on High Pressure Physics, Meriden, New Hampshire, June 1968, personal communication.